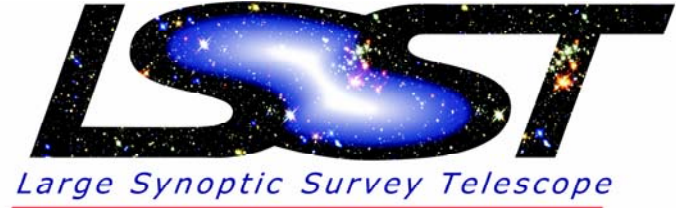


# Probing Dark Energy with Baryon Acoustic Oscillations from the LSST Survey

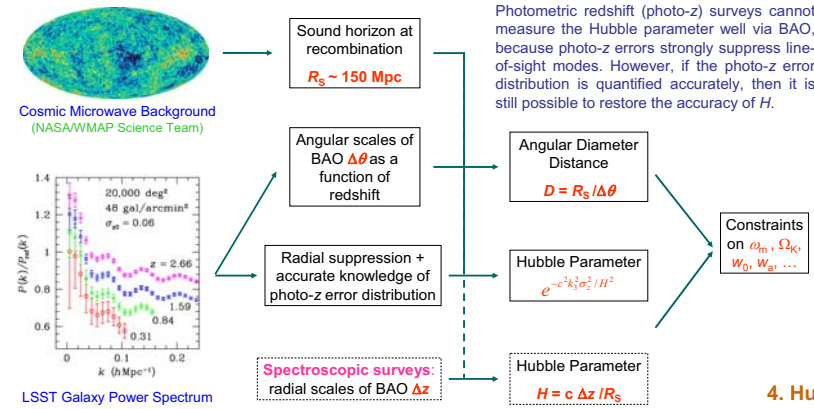
H. Zhan, L. Knox, J.A. Tyson, and V. Margoniner (UC Davis)



The acoustic waves that give rise to the peaks seen in the cosmic microwave background (CMB) temperature fluctuation power spectrum also affect the power spectra of matter and galaxies. The acoustic waves generate a small excess in the galaxy two-point correlation function at roughly 150 Mpc (comoving), corresponding to oscillating features in the power spectra, known as baryon acoustic oscillations (BAO). Since the comoving length scales of these features do not change after recombination, BAO can be used as a CMB-calibrated standard ruler to measure the angular diameter distance and Hubble parameter as functions of redshift. We show that LSST will be able to measure the angular diameter distance to better than a few percent with BAO. Meanwhile, if the distribution of photometric redshift errors is accurately quantified as required by weak lensing, then LSST will also be able to measure the Hubble parameter with a comparable accuracy. This will enable LSST BAO to place constraints on dark energy equation of state parameters that are competitive with those from LSST shear power spectra.

## 1. Baryon Acoustic Oscillations: A Standard Ruler

In the tightly coupled photon-plasma fluid prior to recombination, acoustic waves, supported by the photon pressure, create a characteristic scale – the sound horizon  $R_S$  in matter distribution. Afterward, the sound speed of the neutral gas practically drops to zero, and thus the imprint of  $R_S$  at recombination, e.g. BAO, is frozen (but still evolves gravitationally) in the matter and later galaxy correlation functions. The sound horizon at recombination can be determined accurately with CMB, so that BAO becomes a very promising standard ruler for measuring the angular diameter distance and Hubble parameter (e.g. Eisenstein, Hu, & Tegmark 1998).



## 2. The Survey

LSST will image half of the sky to a limiting magnitude of 26.5 AB mag (see poster 26.01 for more details). For BAO, we divide the survey into 7 redshift bins between  $z = 0.2$  and 3. The galaxy distribution is simply modeled with  $dn/dz = 580 z^2 e^{-z/0.35}$  arcmin<sup>-2</sup>, which results in 48 galaxies per square arcmin within the redshift range. We assume Gaussian photo-z errors with an rms in the form of  $\sigma_z = \sigma_z(1+z)$ .

## 3. Angular Diameter Distance

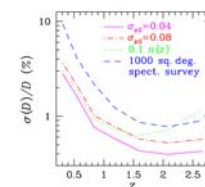


Figure 1. Fractional Errors of the angular diameter distance.

We adopt the method outlined in Seo & Eisenstein (2003) with a few modifications (Zhan & Knox 2005, astro-ph/0509260) to forecast errors on the angular diameter distance  $D$ . Here we assume a flat universe.

With LSST and CMB priors from *Planck*, one can measure  $D$  to sub-percent level (Fig. 1). The large errors at low redshift are due to small volumes and small cutoff wavenumbers of the power spectra that are set to avoid the contamination by nonlinear evolution. The fractional distance errors scale roughly as  $\sqrt{\sigma_z}$ . One may reduce  $\sigma_z$  by only using sub-samples that have better photo-z properties. The case of 0.1  $n(z)$  (dotted line) demonstrates that one gains slightly by trading  $n$  with  $\sigma_z$  at  $z < 1.5$ . For comparison, we also show the results for a 1000 square degree spectroscopic survey (dashed line) that has the same redshift range and binning but with a surface density of 2.3 galaxies per square arcmin.

## 4. Hubble Parameter

The Hubble parameter is a direct measure of the cosmic expansion rate and, hence, crucial for constraining dark energy equation of state (EOS) parameters. Photo-z surveys cannot measure  $H$  accurately through BAO because of the strong photo-z suppression to line-of-sight modes [e.g. by a factor of  $\exp(-c^2 k_{\parallel}^2 \sigma_z^2 / H^2)$  for Gaussian errors]. However, since the suppression is exponentially sensitive to  $H$ , one can achieve tight constraints on  $H$  with accurate knowledge of the photo-z error distribution.

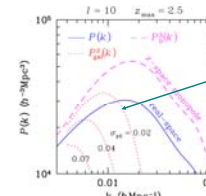


Figure 2. Power spectra.

Galaxy power spectra in spherical harmonic basis with multipole  $l=10$  (Zhan et al. 2006). The suppression is a strong feature that may be used to measure  $H$ , if the photo-z error distribution is known very well.

The constraints on  $H$  (with *Planck* priors and  $\Omega_k=0$ ) is controlled by the prior on  $\sigma_{20}$  in a wide range.

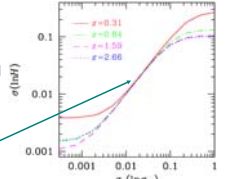


Figure 3. Fractional errors of the Hubble parameter.

## 5. Constraints on Dark Energy Equation of State Parameters

We project the Fisher matrix of the angular diameter distances, Hubble parameters, and other parameters into dark energy parameter space to forecast errors of dark energy EOS parameters  $w_0$  and  $w_a$ , where the EOS  $w$  is parameterized as  $w = w_0 + w_a(1-a)$ . Photo-z error bias and rms are also included as parameters in each redshift bin.

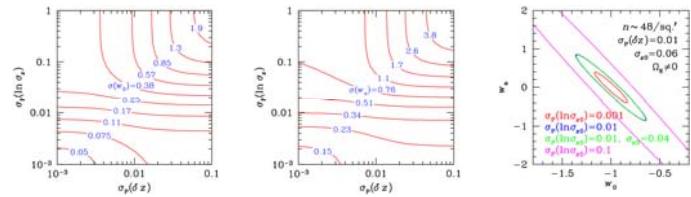


Figure 4. Left panel: Constant-error contours of  $w_0$  as a function of priors on photo-z bias  $\sigma_p(\delta z)$  and rms  $\sigma_p(\ln \sigma_z)$ . Middle panel: The same as the left panel but for  $w_a$ . Right panel:  $1\sigma$  error contours in  $w_0$ - $w_a$  plane.

Fig. 4 demonstrates the improvement of the constraints on  $w_0$  and  $w_a$  with strengthening priors on the photo-z error bias and rms. The left two panels show that, with a prior on the rms photo-z error  $\sigma_p(\ln \sigma_z) \sim 0.01$ , the errors of  $w_0$  and  $w_a$  do not increase much as the prior on the photo-z bias weakens. In other words, BAO can weakly self-calibrate the photo-z bias, given a good prior on the rms. It may also be noted in the right panel of Fig. 4 that a large rms photo-z error is tolerable as long as it is known accurately.

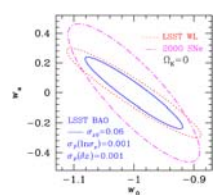


Figure 5. Comparison of BAO, WL, and SNe constraints.

We compare the constraints from LSST BAO, LSST weak lensing (WL) shear power spectra, and *SNAP* 2000 supernovae (SNe) in Fig. 5, assuming  $\Omega_k=0$ . We use strong priors on the photo-z bias and rms to match the WL calculation, which assumes no error in these quantities. Uncertainties in  $\delta z$  and  $\sigma_z$  will degrade WL results (Ma, Hu, & Huterer 2005). Fig. 5 shows that LSST BAO is indeed competitive with the other two techniques in constraining dark energy EOS parameters.

In reality, photo-z errors have long tails due to catastrophic redshift errors. As such, to achieve the tight constraints, one must quantify not only the rms and bias but also the whole distribution of photo-z errors through spectroscopic calibrations and other means.

## 6. Curvature: the Need for High-z Data

It has been shown for type Ia supernova data ( $z < 2$ ) that the constraints on dark energy EOS parameters can loosen considerably if one relaxes the flatness assumption (Weller & Albrecht 2001; Linder 2005). The reason is that curvature is somewhat degenerate with dark energy. For example, it is indistinguishable from dark energy of  $w = -1/3$  in terms of  $D$  and  $H$ . The equivalent energy fraction due to curvature,  $\Omega_k$ , evolves as  $(1+z)^2$ , so one can constrain it better with high- $z$  data (assuming as usual that dark energy evolves much slower) and partially restore the constraints on dark energy EOS parameters.

For LSST BAO with the flatness assumption, high- $z$  data ( $z > 1.4$ ) do not provide much additional constraint on dark energy EOS parameters  $w_0$  and  $w_a$  (see Fig. 6). However, with  $\Omega_k$  being a free parameter, the errors on  $w_0$  and  $w_a$  increase by 45% and 65%, respectively, if the three  $z > 1.4$  bins are not available. Hence, high- $z$  data are useful for breaking the degeneracy between curvature and dark energy. In this example, LSST BAO constrains  $\Omega_k$  to  $\pm 10^{-3}$ .

For a much-smaller-volume survey the constraints on  $w_0$  and  $w_a$  can degrade severely even with the flatness assumption if there is no high- $z$  data.

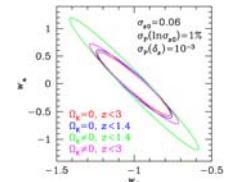


Figure 6. Effect of curvature and high- $z$  data on  $w_0$  and  $w_a$ .

The LSST research and development effort is funded in part by the National Science Foundation under Scientific Program Order No. 9 (AST-0551161) through Cooperative Agreement AST-0132798. Additional funding comes from private donations, in-kind support at Department of Energy laboratories and other LSSTC Institutional Members.

National Optical Astronomy Observatory  
Research Corporation  
The University of Arizona  
University of Washington

Brookhaven National Laboratory  
Harvard-Smithsonian Center for Astrophysics  
Johns Hopkins University  
Las Cumbres Observatory, Inc.

Lawrence Livermore National Laboratory  
Stanford Linear Accelerator Center  
Stanford University  
The Pennsylvania State University

University of California, Davis  
University of Illinois at Urbana-Champaign